13
Worst Imperfection for Stable Bifurcation

13.1 Introduction

The procedures to determine the worst mode of imperfection presented in Chapters 11 and 12 are pertinent design methodologies for structures undergoing unstable bifurcation such as cylindrical shells and stiffened plates. However, these methodologies malfunction for a stable-symmetric bifurcation point, because this point on the fundamental path disappears in the presence of a major imperfection.

Let us observe the equilibrium paths for major and minor imperfections illustrated in Fig. 13.1. For a major imperfection, Λ increases above the bifurcation load factor Λ^{c} of the perfect system (cf., Fig. 13.1(a)). For a minor imperfection, an imperfect system retains a bifurcation point, and the bifurcation load factor may increase or decrease depending on the sign of the imperfection parameter (cf., Fig. 13.1(b)).

A question arises whether it is safe to allow loads above the bifurcation load Λ^{c}. From a sole standpoint of stability, it seems possible to allow the loading along the bifurcation path exceeding the bifurcation load [246], and to determine the maximum load factor by constraints on displacements and/or stresses. For example, optimal design that has a stable-symmetric bifurcation point can be found by constraining the fourth-order differential coefficient $V_{,1111}$ to be nonnegative ($V_{,1111} \geq 0$) [31, 32, 97, 246].

Although a critical point does not exist for a structure with a major imperfection, the structure may undergo sudden dynamic large antisymmetric deformation near the stable bifurcation point as the load factor is further increased. The occurrence of such sudden deformation becomes abrupt if the major imperfection is extremely small.

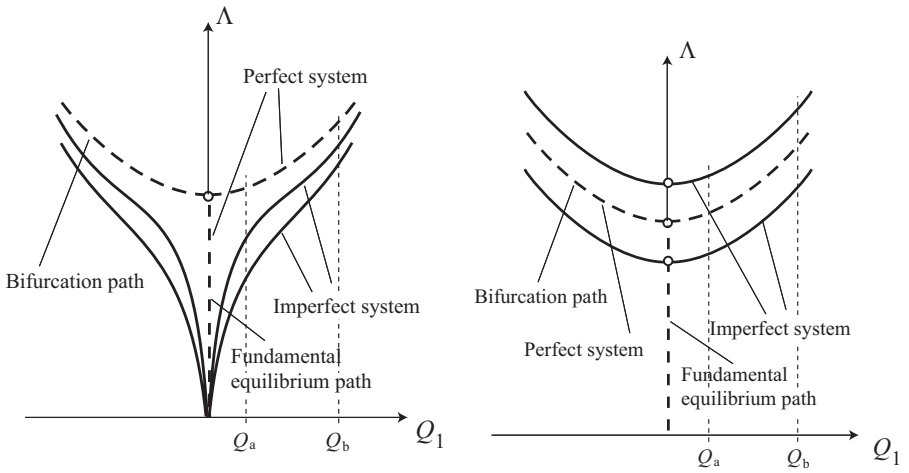

(a) Major imperfection (b) Minor imperfection

Fig. 13.1 Equilibrium paths of perfect and imperfect systems. ○: bifurcation point; Q_1: generalized displacement in the direction of bifurcation mode; solid curve: perfect equilibrium path; dashed curve: imperfect equilibrium path.

In this chapter, a simple and numerically efficient procedure is presented for determining the maximum load factor of an imperfect elastic structure undergoing stable bifurcation for minor imperfections of nodal locations. We consider a flexible structure allowing moderately large deformation. An anti-optimization problem is formulated so as to minimize the bifurcation load factor within the convex bounds on imperfection parameters. The method called *simultaneous analysis and design* (SAND) [104, 315] is used, for which imperfections of nodal loads are introduced, and the displacements are also considered as independent variables to avoid costly nonlinear path-tracing analysis. It is shown for a plane column-type truss that the worst mode of imperfection, which turns out to be a minor imperfection, can be successfully obtained by the present approach.

This chapter is organized as follows. A procedure for determining the maximum load factor is introduced in Section 13.2. An anti-optimization problem is formulated in Section 13.3. The worst imperfections of column-type trusses are studied in Section 13.4.

13.2 Maximum Load Factor for Stable Bifurcation

The maximum load factor of a structure exhibiting stable bifurcation may be defined by either bifurcation load factor Λ^{c}, or the load factor Λ^{M} to be defined in accordance with the specified bounds on stresses and/or displacements.

The worst imperfection to be obtained changes according to whether Λ^{c} or Λ^{M} is employed. First, if the bifurcation load factor Λ^{c} is used, the worst imperfection

should be a minor imperfection because the bifurcation point exists for a minor imperfection but disappears for a major imperfection.

Next we use the maximum load factor Λ^{M} that is defined by the upper-bound constraint $Q_1 \le Q_1^{\mathrm{U}}$ of the generalized displacement Q_1 in the direction of the bifurcation mode. As illustrated in Fig. 13.1, the reduction of Λ^{M} due to a major imperfection is very large for a relatively strict constraint $Q_1^{\mathrm{U}} = Q_{\mathrm{a}}$, but becomes smaller as Q_1^{U} is relaxed to, e.g., $Q_1^{\mathrm{U}} = Q_{\mathrm{b}}$.

For a minor imperfection, as can be observed from Fig. 13.1(b), the amount of reduction is not sensitive to Q_1^{U}, and the sensitivity of the maximum load to a minor imperfection is almost equivalent to that of the bifurcation load. The reduction is larger than that for a major imperfection if Q_1^{U} is moderately large, e.g., $Q_1^{\mathrm{U}} = Q_{\mathrm{b}}$. Therefore, the worst mode of imperfection for Λ^{M} corresponds to the major imperfection for small Q_1^{U}, and to the minor imperfection for large Q_1^{U}.

Thus, for a flexible structure allowing moderately large deformation, a minor imperfection plays a key role in defining both load factors Λ^{c} and Λ^{M}, and the maximum load defined by deformation constraints may be dramatically reduced by minor imperfections rather than by major imperfections. For this reason, we consider worst minor imperfections of the bifurcation load in the remainder of this chapter.

13.3 Anti-Optimization Problem

An anti-optimization problem for minimizing the bifurcation load factor Λ^{c} against a minor imperfection is formulated.

Consider an imperfection pattern vector $\mathbf{d} \in \mathbb{R}^{\nu}$ for, e.g., nodal locations and cross-sectional areas. The norm of $\mathbf{d}$ is denoted by $\|\mathbf{d}\|_H^2 = \mathbf{d}^{\top}\mathbf{H}\mathbf{d}$ for a positive-definite weight matrix $\mathbf{H}$, and $\|\mathbf{d}\|_H^2$ is a convex function of $\mathbf{d}$.

13.3.1 Direct formulation

Specify an upper bound $\overline{\|\mathbf{d}\|_H^2}$ for $\|\mathbf{d}\|_H^2$. Decompose the imperfection mode $\mathbf{d}$ into major imperfection $\mathbf{d}^+$ and minor imperfection $\mathbf{d}^-$. The maximum load of an imperfect system considering reduction by the worst mode of a minor imperfection is defined as the solution of the following anti-optimization problem:

$$\text{AP1:} \quad \text{minimize} \quad \Lambda^{\mathrm{c}}(\mathbf{d}^-) \tag{13.1a}$$

$$\text{subject to} \quad \|\mathbf{d}^-\|_H^2 \le \overline{\|\mathbf{d}^-\|_H^2} \tag{13.1b}$$

Problem AP1 may be solved by using an appropriate gradient-based optimization algorithm if sensitivity coefficients of Λ^{c} can be computed. However, AP1 is computationally expensive, because Λ^{c} for a given $\mathbf{d}^-$ should be determined by path-tracing analysis at each iterative step of optimization.

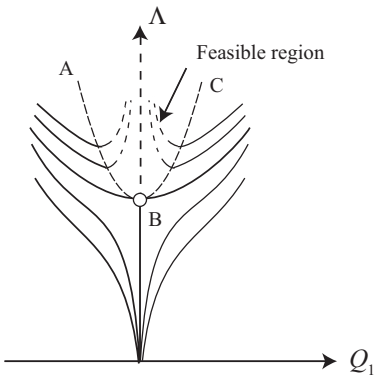

Fig. 13.2 Feasible region for the eigenvalue constraint $\lambda_1 \leq 0$. Solid curve: stable; dashed curve: unstable; ○: stable bifurcation point.

13.3.2 Numerically efficient formulation

A numerically efficient formulation to find Λ^{c} as the minimum value of Λ under constraint $\lambda_1 \leq 0$ is presented.

If we fix $\mathbf{d}^-$ and only consider a major imperfection $\mathbf{d}^+$, the feasible region in the (Q_1, Λ)-space satisfying $\lambda_1 \leq 0$ lies above the curve ABC in Fig. 13.2. For stable bifurcation under consideration, the feasible region in the vicinity of the bifurcation point is convex in the (Q_1, Λ)-space. Hence, the bifurcation load of the imperfect system for a minor imperfection is found by the two steps of minimization:

Step 1: Minimize Λ with respect to $\mathbf{d}^+$ under constraint of $\lambda_1 \leq 0$ to find the bifurcation load Λ^{c}.

Step 2: Minimize $\Lambda = \Lambda^{\mathrm{c}}$ with respect to $\mathbf{d}^-$ to obtain the worst imperfection.

Since both steps correspond to minimization of Λ, they can be carried out by considering major and minor imperfections simultaneously as variables.

The method called *simultaneous analysis and design*, which is abbreviated as SAND, is very efficient for reducing the required number of path-tracing analyses that are to be carried out at each step of optimization or anti-optimization of geometrically nonlinear structures. The state variable vector $\mathbf{U}$, as well as the design variables, are considered as independent variables [104, 315].

To utilize SAND, we consider the nodal displacement vector $\mathbf{U}$ as independent variables in addition to $\mathbf{d}$. In the conventional formulation of SAND, $\mathbf{U}$ is modified to satisfy the equilibrium equations, or to minimize the total potential energy. In order to make it easier to solve the optimization problem, AP1 in (13.1a) and (13.1b) is relaxed by permitting imperfections in nodal loads, because in our problem for obtaining the worst imperfection it is not very important to employ exactly *perfect* nodal loads. The ranges of the nodal loads Λp_i are given as

$$\Lambda p_i^{\mathrm{L}} \leq \Lambda p_i \leq \Lambda p_i^{\mathrm{U}}, \quad (i = 1, \ldots, n) \tag{13.2}$$

where p_i^{L} and p_i^{U} are the specified lower and upper bounds, respectively, and n is the number of degrees of freedom.

Suppose the case where the errors in the loads are bounded by $\pm\Lambda\Delta p$, and rewrite (13.2) into

$$\Lambda(p_i^0 - \Delta p) \le \Lambda p_i \le \Lambda(p_i^0 + \Delta p), \quad (i = 1, \ldots, n) \tag{13.3}$$

where p_i^0 is the perfect value of p_i.

The equivalent nodal load $R_i(\mathbf{U}, \mathbf{d})$ $(i = 1, \ldots, n)$ in the direction of U_i of an imperfect system is then calculated for current values of $\mathbf{U}$ and $\mathbf{d}$ during anti-optimization. Recall that R_i is the derivative of the strain energy for the proportional loading (cf., (1.11) with $R_i = H_{,i}$ in Section 1.2).

The anti-optimization problem for finding the minimum $\Lambda^{\min}$ of Λ under constraints on the norms of imperfections and the sign of the lowest eigenvalue $\lambda_1(\mathbf{U}, \mathbf{d})$ of the tangent stiffness matrix is formulated as

$$\begin{aligned}
\text{AP2:}\quad & \text{minimize} && \Lambda && (13.4a)\\
& \text{subject to} && \|\mathbf{d}\|_H^2 \le \overline{\|\mathbf{d}\|_H^2} && (13.4b)\\
& && \Lambda(p_i^0 - \Delta p) \le R_i(\mathbf{U}, \mathbf{d}) \le \Lambda(p_i^0 + \Delta p), \quad (i = 1, \ldots, n) && (13.4c)\\
& && \lambda_1(\mathbf{U}, \mathbf{d}) \le 0 && (13.4d)\\
& && U_i^{\mathrm{L}} \le U_i \le U_i^{\mathrm{U}}, \quad (i = 1, \ldots, n) && (13.4e)
\end{aligned}$$

The variables of this problem are $\mathbf{U}, \mathbf{d}$ and Λ, and the upper- and lower-bound constraints (13.4e) are assigned for $\mathbf{U}$ to improve convergence. Only $R_i(\mathbf{U}, \mathbf{d})$ $(i = 1, \ldots, n)$ and $\lambda_1(\mathbf{U}, \mathbf{d})$ are to be computed for the current values of $\mathbf{U}$ and $\mathbf{d}$ at each iterative step of optimization without resort to costly path-tracing analysis.

13.4 Worst Imperfection of Column-Type Trusses

Consider the plane column-type truss as shown in Fig. 13.3. The two springs attached at nodes 7 and 8 have the same extensional stiffness K. We consider two cases

- *column-type truss* with $K = 0$, and
- *laterally supported truss* with $K \neq 0$.

The lengths of x- and y-directional members are 1000 mm and 2000 mm, respectively. All the truss members have the same cross-sectional area of 200.0 mm^2. The proportional loads Λp in the negative y-direction are applied at nodes 7 and 8, where $p = 98$ kN. Young's modulus is $E = 205.8\ \mathrm{kN/mm}^2$. The axial strain is defined by Green's strain. The units of force kN and of length mm are suppressed in the following.

Optimization problem AP2 is solved by IDESIGN Ver. 3.5 [14], in which the SQP (cf., Section 4.3.2) is used, and the gradients of the objective and constraint functions are computed by the finite difference approach.

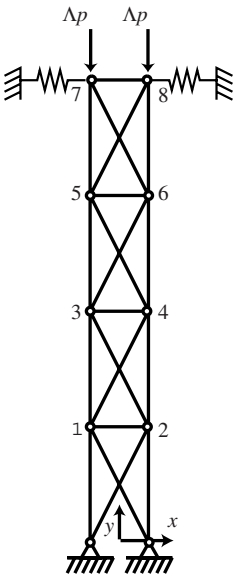

Fig. 13.3 Column-type plane truss.

The components of the imperfection pattern vector consist of the coordinates of all the nodes except for the two supports. Therefore, the size of $\mathbf{d}$ is equal to $n\ (=16)$. The weight matrix is given as $\mathbf{H} = (1/n^2)\mathbf{I}_n$, where $\mathbf{I}_n \in \mathbb{R}^{n\times n}$ is the identity matrix. The upper bound for the error in the nodal loads is $\Delta p = 0.98$. The total number of variables $\mathbf{d}, \mathbf{U}$ and Λ in AP2 is 33. The upper and lower bounds, which are given as $U_i^{\mathrm{L}} = -3000$ and $U_i^{\mathrm{U}} = 3000$ for U_i, are inactive for the following anti-optimal solutions.

Let $\mathbf{\Phi}^+$ and $\mathbf{\Phi}^-$ denote the lowest antisymmetric and symmetric linear buckling modes of the perfect system, respectively. Imperfection sensitivity is investigated for the major imperfections in the directions of $\mathbf{\Phi}^+$ and the minor ones in the direction of $\mathbf{\Phi}^-$, in comparison with the worst imperfection. Since the prebuckling deformation is not very large for the perfect column-type trusses, the eigenmode associated with the null eigenvalue of the tangent stiffness matrix at the critical point can be approximated by a linear buckling mode.

13.4.1 Column-type truss

Consider the column-type truss ($K = 0$). The critical load factor of the perfect system is $\Lambda^{\mathrm{c}0} = 3.9366$ at a stable-symmetric bifurcation point with a bifurcation mode that is antisymmetric with respect to the y-axis.

We first investigate imperfection sensitivity of the maximum load factor in the directions of $\mathbf{\Phi}^+$ and $\mathbf{\Phi}^-$ shown in Figs. 13.4(a) and (b), respectively. Let U_x denote the x-directional displacement of node 8, and Fig. 13.5 shows equilibrium paths for the perfect and imperfect systems with major imperfections in the direction of $\mathbf{\Phi}^+$ with $\|\mathbf{d}\|_H^2 = 10^2$ and 50^2. As is seen, Λ increases very slightly

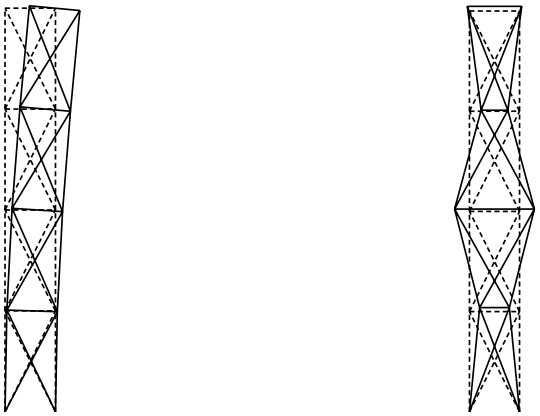

(a) Antisymmetric mode $\mathbf{\Phi}^+$ (b) Symmetric mode $\mathbf{\Phi}^-$

Fig. 13.4 Lowest symmetric and antisymmetric linear buckling modes of the column-type truss.

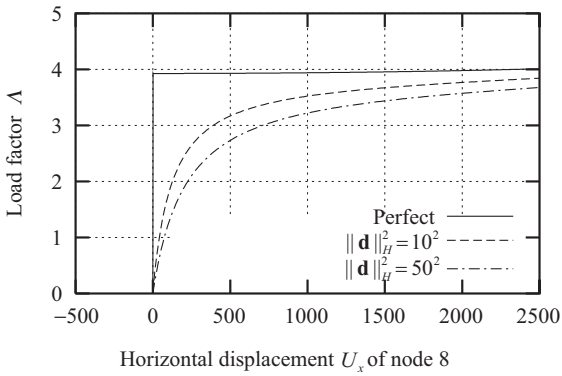

Fig. 13.5 Equilibrium paths for perfect and imperfect column-type trusses with major imperfections in the direction of $\mathbf{\Phi}^+$.

along the bifurcation path for the perfect system. Fig. 13.6 shows the paths for minor imperfections corresponding to $\mathbf{\Phi}^-$ with $\|\mathbf{d}\|_H^2 = 10^2$ and 50^2.

Define the maximum load factor Λ^{M} by the displacement constraint $U_x \le \overline{U}_x$. It may be observed from Figs. 13.5 and 13.6 that the reduction of Λ^{M} due to a major imperfection is larger than that to a minor imperfection for small $\overline{U}_x$, but a minor imperfection is more influential than a major imperfection for sufficiently large $\overline{U}_x$. For instance, for $\|\mathbf{d}\|_H^2 = 50^2$, the reduction for a minor imperfection is larger than that for a major imperfection in the range $U_x > 1790$. It is to be emphasized, for minor imperfections, that the amount of reduction of Λ^{M} does not strongly depend on the value of $\overline{U}_x$. Therefore, the worst minor imperfection mode for Λ^{M} can be successfully obtained by solving AP2 that minimizes the bifurcation load.

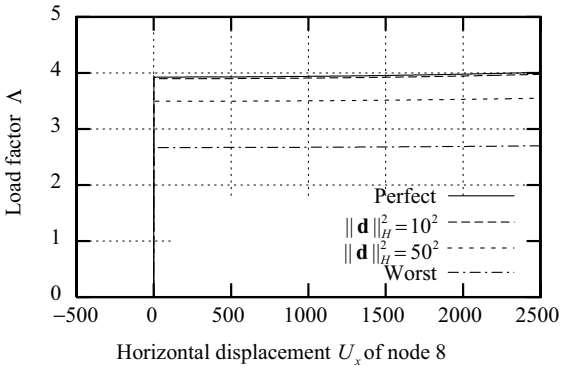

Fig. 13.6 Equilibrium paths for perfect and imperfect column-type trusses with minor imperfections in the direction of $\mathbf{\Phi}^-$.

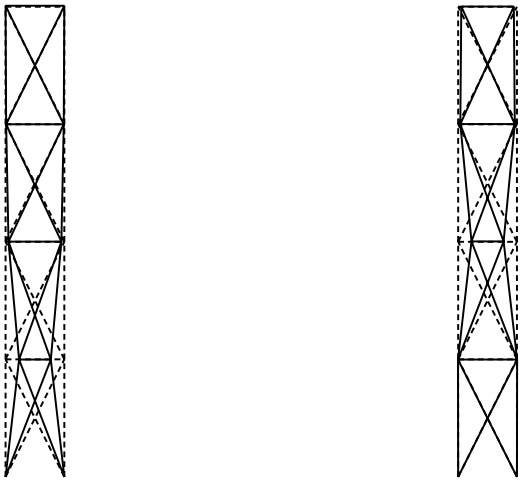

(a) Column-type truss ($K = 0$) (b) Laterally supported truss ($K \neq 0$)

Fig. 13.7 Worst modes of imperfection.

The minimum of Λ of AP2 for $\|\mathbf{d}\|_H^2 \leq \overline{\|\mathbf{d}\|_H^2} = 50^2$ is $\Lambda^{\min} = 2.6693$, which is about 68% of $\Lambda^{c0} = 3.9366$ of the perfect system. The worst mode of nodal imperfection $\mathbf{d}^\perp$ is as shown in Fig. 13.7(a), which is symmetric with respect to the y-axis and corresponds to a minor imperfection. The worst imperfections of nodal locations and nodal loads are also listed in Table 13.1; all the components of $\Delta\mathbf{p} = \mathbf{p} - \mathbf{p}^0$ are equal to the upper or lower bound. The equilibrium path for the worst imperfection is plotted in Fig. 13.6 by the dotted-dashed line.

Note that Λ^c of the imperfect system corresponding to $\|\mathbf{d}\|_H^2 = 50^2$ in the direction of $\mathbf{\Phi}^-$ is 3.4747, which is much larger than that for the worst imperfection $\mathbf{d}^\perp$. Therefore, $\mathbf{\Phi}^-$ cannot be used to approximate $\mathbf{d}^\perp$.

Table 13.1 Worst imperfections of nodal locations and nodal loads.

Node	Direction	Location	Load ($\Delta p_i/\|p\|$)
1	x	137.81	0.01
	y	−2.2715	−0.01
2	x	−137.83	−0.01
	y	−2.2766	−0.01
3	x	29.410	0.01
	y	2.2275	−0.01
4	x	−29.375	−0.01
	y	2.2211	−0.01
5	x	6.8235	0.01
	y	0.13910	−0.01
6	x	−6.8769	−0.01
	y	0.11772	−0.01
7	x	−0.49643	0.01
	y	9.1936	−0.01
8	x	0.49153	−0.01
	y	9.1907	−0.01

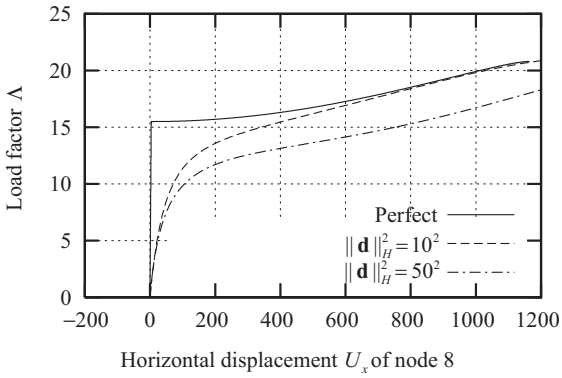

Fig. 13.8 Equilibrium paths for perfect and imperfect laterally supported trusses with major imperfections in the direction of $\mathbf{\Phi}^+$.

13.4.2 Laterally supported truss

Consider next a laterally supported truss with $K = 0.1029$. The ratio of the extensional stiffness of the spring to that of the horizontal truss member is 0.005. The critical load factor of the perfect system is $\Lambda^{c0} = 15.497$.

Fig. 13.8 shows equilibrium paths for major imperfections corresponding to $\mathbf{\Phi}^+$ with $\|\mathbf{d}\|_H^2 = 10^2$ and 50^2. As is seen, the critical point of the perfect system is a stable-symmetric bifurcation point, and the critical loads Λ^c of imperfect systems are far above the bifurcation load. Note that, under displacement constraint of a moderately large upper bound, the reduction of the maximum load Λ^M of the

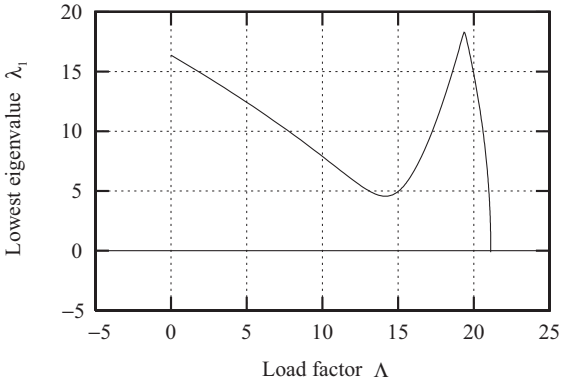

Fig. 13.9 Relation between load factor Λ and the lowest eigenvalue λ_1 with $\|\mathbf{d}\|_H^2 = 10^2$.

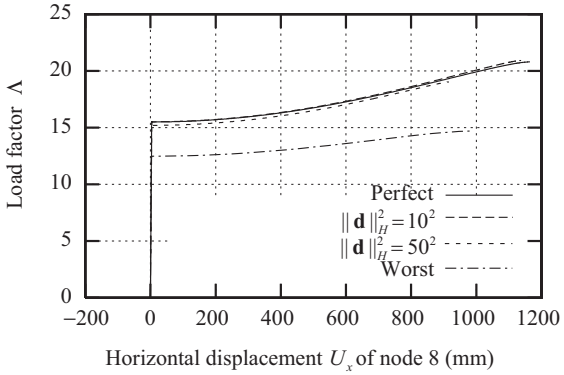

Fig. 13.10 Equilibrium paths for perfect and imperfect laterally supported trusses with minor imperfections in the direction of $\mathbf{\Phi}^-$.

imperfect system from that of the perfect system is very small for $\|\mathbf{d}\|_H^2 = 10^2$. Variation of λ_1 with respect to Λ for $\|\mathbf{d}\|_H^2 = 10^2$ is as shown in Fig. 13.9. The lowest eigenvalue has a local minimum at $\Lambda \simeq 14.5$ near the bifurcation point of the perfect system, but does not reach 0.

Fig. 13.10 shows equilibrium paths for minor imperfections in the direction of $\mathbf{\Phi}^-$ with $\|\mathbf{d}\|_H^2 = 10^2$ and 50^2. Note that the bifurcation load factor for $\|\mathbf{d}\|_H^2 = 50^2$ is 14.107, where imperfections in nodal loads in the direction of $\mathbf{\Phi}^-$ are also considered.

The load factor of the worst imperfection obtained by solving AP2 for $\|\mathbf{d}\|_H^2 \leq \overline{\|\mathbf{d}\|_H^2} = 50^2$ is $\Lambda^{\min} = 12.483$ which is about 81% of $\Lambda^{\mathrm{c}} = 15.497$ of the perfect system. The equilibrium path for the worst imperfection $\mathbf{d}^{\perp}$, which has reflection symmetry as shown in Fig. 13.7(b), is also plotted in Fig. 13.10. In this case the reduction of Λ^{M} due to the worst imperfection is much larger than that to the

imperfection with the same norm in the direction of $\mathbf{\Phi}^{-}$. Note from Fig. 13.7 that $\mathbf{d}^{\perp}$ strongly depends on the presence of the extensional stiffness of the spring.

13.5 Summary

In this chapter,

- the maximum load factor for stable bifurcation based on displacement constraint has been defined,
- an anti-optimization problem for minimizing the critical load factor has been formulated, and
- the worst imperfection of a column-type plane truss has been studied.

The major findings of this chapter are as follows.

- The critical point of an imperfect system disappears if the perfect system has a stable-symmetric bifurcation point. In this case, the maximum load may be defined in reference to displacements and stresses of imperfect systems with a specified norm of the worst imperfection.
- The worst minor imperfection can be successfully obtained as a solution of an anti-optimization problem under a constraint on the lowest eigenvalue of the tangent stiffness matrix. The problem is relaxed incorporating imperfections of nodal loads and is solved by employing nodal displacements as independent variables without resort to costly path-tracing analysis at each step of anti-optimization.
- For a flexible structure allowing moderately large displacements, the anti-symmetric buckling mode is not always the worst mode of imperfection and that a minor imperfection is very important for estimating the reduction of the maximum load factor defined by displacement constraints.